Journal of Statistical Physics, Vol. 68, Nos. 1/2, 1992

Semiclassical Wavefunctions of Nonintegrable Systems and Localization on Periodic Orbits

D. C. Meredith[1]

Received December 9, 1991; final March 6, 1992

We review semiclassical approximations for wavefunctions, including the EBK approximation for integrable systems and the recent work of Bogomolny and Berry for nonintegrable systems, stemming from the periodic orbit theory of Gutzwiller and Balian and Block. In particular we focus on the localization around periodic orbits (scarring) first appreciated by Heller, and the description of this scarring in both coordinate and phase space. We examine individual wavefunctions of a schematic shell model in phase space and find that few are ergodic. We also find that the degree of localization depends both on the degree of chaos in the classical limit and on the nearness of the eigenvalue to an energy that quantizes the scarring periodic orbit.

KEY WORDS: Semiclassical wavefunctions; periodic orbit theory; scarred wavefunctions; EBK approximation; schematic shell model; Wigner distribution; Husimi distribution.

Dynamical chaos in classical mechanics is described as "instability with respect to initial conditions." There is evidence[1] that such instability does not occur in the analogous quantum mechanical problems. However, there is no doubt that the qualitative change in the classical dynamics is reflected in a similar change in the quantum mechanics. To appreciate this change, first consider the simple one-dimensional, time-independent (and therefore nonchaotic) system. Classically, the motion in phase space is confined to one-dimensional isoenergy surface and is completely predictable. Quantum mechanically, the WKB approximation provides a good approximation to the energy eigenvalues and eigenfunctions; we do not need to solve the time-independent Schrödinger equation to know where the probability is the largest. On the other hand, if we consider a classical system that is

[1] Physics Department, University of New Hampshire, Durham, New Hampshire.

822/68/1-2-7

chaotic, the dynamics is unpredictable, while in the quantum regime the WKB method no longer applies. Does that mean we lost all ability to say something about the probability short of doing the calculations? Has the classical mechanics ceased being of any use in solving the quantum mechanics?

The answer, fortunately, is no. One approach to this problem of quantum mechanics of chaotic systems is periodic orbit theory, developed by Gutzwiller[2] and Balian and Bloch.[3] They derived an alternate quantization procedure (which works regardless of the degree of chaos in the classical limit) which expresses the density of states as a sum over all periodic orbits. More recently, it has been found that periodic orbits also influence the wavefunctions. Heller[4] found that the short unstable periodic orbits give rise to a localization of the eigenvectors, known as scarring. Heller's work has sparked much theoretical and numerical work on wavefunctions in the context of periodic orbit theory.

This paper is concerned with semiclassical energy eigenfunctions in general, and with scarring in particular. Section 1 begins with a general review of semiclassical wavefunctions, including some background on classical dynamics; Section 2 describes wavefunctions in phase space; Section 3 describes the initial work concerning semiclassical wavefunctions of nonintegrable systems; Section 4 relates the initial discovery of scarred eigenfunctions; Section 5 discusses recent work on scars in the context of periodic orbit theory; and Section 6 gives a brief summary of current work on scars. Section 7 introduces our model Hamiltonian, and Section 8 explores scarring in this system, with particular attention given to individual states and their quantal surfaces of section.

As a final general remark, we note that interested readers may turn to the excellent reviews by Berry[5] and Berry and Mount[6] for in-depth discussions of semiclassical methods, to the wealth of recently published books on the classical and quantum mechanics of nonintegrable systems (for general references on both classical and quantum Hamiltonian chaos see refs. 7), and to several books on classical mechanics that treat nonintegrable systems in depth (see refs. 8 for treatments of classical Hamiltonian dynamics that include nonintegrable systems).

1. SEMICLASSICAL WAVEFUNCTIONS OF INTEGRABLE SYSTEMS

We begin with integrable systems, i.e., those for which the number of degrees of freedom equals the number of constants of the motion. These constants must be linearly independent and in involution (i.e., the Poisson bracket for each pair is zero). In the semiclassical limit, a great deal is

known about the wavefunctions of these systems because the classical dynamics is beautifully simple.[7,8] This simplicity arises because in phase space (where the variables are momenta and coordinates) classical trajectories are confined to N-dimensional tori[9] (i.e., an N-dimensional cube with periodic boundary conditions) which are therefore invariant under the dynamics. Because phase space is foliated by tori, there exists a canonical change of coordinates such that the Hamiltonian can be written as a function of the new momenta alone; these momenta are known as the actions $\mathbf{I}$. Using Hamilton's equations of motion, we find that the actions are constant in time and that the conjugate coordinates, the angles $\boldsymbol{\theta}$, change linearly in time. Therefore in these systems the dynamics is trivial; however, finding the constants of the motion (or knowing if they exist) becomes the difficult task.

This organization of classical phase space (i.e., the foliation by tori) is necessary for the Einstein–Brillouin–Keller (EBK) approximation, which is the generalization to higher dimensions of the better known Wentzel–Kramers–Brillouin (WKB) approximation for one-dimensional problems[5–7] and was introduced for general systems by Van Vleck.[10] The key to this method is the association of an invariant torus with a wavefunction in such a way that the association persists in time. Since the torus is invariant with time, so is the wavefunction, and therefore the wavefunction is an energy eigenfunction. The association is made as follows: the amplitude of the wavefunction is the square root density of points evenly distributed on the torus, projected onto coordinate space, and the phase is given by the action

$$S(\mathbf{q}, \mathbf{I}) = \int_{\mathbf{q}_0}^{\mathbf{q}} \mathbf{p}(\mathbf{q}', \mathbf{I}) \cdot d\mathbf{q}' \tag{1}$$

The complete wavefunction is the sum of several such terms:

$$\Psi_{\mathrm{sc}}(\mathbf{q}) = \sum_{\text{branches } n} \left| \det \frac{\partial^2 S_n}{\partial q_j \, \partial I_k} \right|^{1/2} \exp\left(\frac{i S_n(\mathbf{q}, \mathbf{I})}{\hbar} - \frac{i\mu\pi}{2} \right) \tag{2}$$

one for each branch of $\mathbf{p}(\mathbf{q}, \mathbf{I})$.

The last term in the exponential ($i\mu\pi/2$) arises from careful consideration of the turning points in coordinate space (caustics) where the amplitude diverges and the values from the different branches must join smoothly. The details were worked out by Maslov,[11] who repeated the same procedure as above for the wavefunction in momentum space (whose caustics cannot be the same as those in coordinate space), then related the two wavefunctions via Fourier transforms, and thereby determined the correct phase difference between the different branches (this work is

reviewed in ref. 12). The Maslov index μ included in the phase changes by integer amounts at conjugate points (i.e., those places where the amplitude diverges).

Finally, the quantization of energy arises when we require that the wavefunction be single-valued, for which we obtain

$$\oint_{C_k} \mathbf{p}(\mathbf{q}, \mathbf{I}) \cdot d\mathbf{q} = 2\pi\hbar \left(n_k + \frac{\mu_k \pi}{2} \right) \equiv 2\pi I_k \tag{3}$$

where C_k is the kth irreducible circuit around the torus, and I_k is the quantized action.

2. QUANTUM MECHANICS AND PHASE SPACE

So far, we have obtained the semiclassical wavefunction in coordinate representation. Coordinate space, however, is not as informative as phase space: in phase space, trajectories do not intersect, the flow is volume-preserving, and the invariant structures (e.g., tori) are unambiguously identifiable. It is reasonable to expect that quantum mechanics in phase space could also be more enlightening. In this section we will examine ways to express quantum mechanics in phase space.

To express a wavefunction in terms of both $\mathbf{q}$ and $\mathbf{p}$ we begin with the Weyl transform of an arbitrary quantum operator $\hat{A}$, defined as follows:

$$W_{\hat{A}}(\mathbf{q}, \mathbf{p}) \equiv \frac{1}{(2\pi\hbar)^N} \operatorname{Tr} \left(\hat{A} \int d\mathbf{Q}\, d\mathbf{P} \right.$$
$$\left. \times \exp \left\{ \frac{i}{\hbar} [(\hat{\mathbf{p}} - \mathbf{p}) \cdot \mathbf{Q} + (\hat{\mathbf{q}} - \mathbf{q}) \cdot \mathbf{P}] \right\} \right) \tag{4}$$

where N is the number of degrees of freedom. This transforms any quantum operator into a function of $\mathbf{q}$ and $\mathbf{p}$. Therefore, to obtain a function for a wavevector in phase space, it is reasonable to take $\hat{A} = |\Psi\rangle\langle\Psi|/(2\pi\hbar)^N$. This is known as the Wigner function[13] of Ψ (see ref. 14 for examples). After some manipulation, this is written in the more familiar form

$$W_\Psi(\mathbf{q}, \mathbf{p}) = (2\pi\hbar)^{-N} \int d\mathbf{q}' \exp(-i\mathbf{p} \cdot \mathbf{q}'/\hbar)\, \Psi^*(\mathbf{q} - \mathbf{q}'/2)\, \Psi(\mathbf{q} + \mathbf{q}'/2) \tag{5}$$

The Wigner function can become negative, so it is not a probability density in phase space. However, we can recover the usual probabilities from W_Ψ: the Wigner function integrated over $\mathbf{p}$ gives the probability in coordinate space, while the integral over $\mathbf{q}$ gives the probability in momentum space.

As an example, consider the semiclassical wavefunction for integrable systems derived in Eq. (2); the corresponding Wigner function can be calculated via the stationary phase approximation.[5] The distribution is a delta function on the corresponding quantized torus,

$$W_{\mathbf{k}}(\mathbf{q}, \mathbf{p}) = \frac{1}{(2\pi)^N} \delta(\mathbf{I}(\mathbf{q}, \mathbf{p}) - \mathbf{I}_{\mathbf{k}}) \tag{6}$$

where $\mathbf{I}_{\mathbf{k}}$ are the quantized actions (3). This is precisely as we might expect given the method of construction of (2). Therefore, although this method of moving into phase space is not unique, it gives semiclassical results in agreement with classical intuition.

Another method to lift the wavefunction into phase space is the Husimi distribution,[15] defined as the overlap between a coherent state and the wavefunction:

$$\mathscr{H}_{\Psi}(\mathbf{q}, \mathbf{p}) = |\langle \mathbf{q}, \mathbf{p} \mid \Psi \rangle|^2 \tag{7}$$

where coherent states $|\mathbf{q}, \mathbf{p}\rangle$ are defined as the minimum-uncertainty wave packet,[16] i.e., a "quantum point." For the Heisenberg–Weyl group $(\hat{x}, \hat{p}, \hat{1})$, the coherent state is a Gaussian wave packet, parametrized by the center of the packet $\mathbf{p}, \mathbf{q}$. Although Gaussians are the best known coherent states, they are not the only ones. Many other dynamical symmetry groups also have their own appropriate coherent states,[16] and therefore this procedure for moving into phase space is applicable to eigenstates of many Hamiltonians.

The advantage of the Husimi over the Wigner distribution is that the Husimi is everywhere positive and does not display the rapid oscillations characteristic of the Wigner.[17] On the other hand, there is arbitrariness in the coherent states (and therefore the Husimi) because the uncertainty is split arbitrarily between $\mathbf{q}$ and $\mathbf{p}$. However, one serious objection to Husimis has been recently removed. It was at first thought that phase information was lost in taking the square of the overlap. However, Leboeuf and Voros[18] have pointed out that all the information about Ψ is retained in the Husimi via its zeros since the Husimi is an analytic function.

Now we have two ways of evaluating wavefunctions in phase space, but there are still technical difficulties with plotting. If we have two degrees of freedom, phase space is four-dimensional, and the energy shell is three-dimensional; neither can be easily be plotted on paper. The solution is known as a surface of section. Classically, these are created by fixing one variable (e.g., $q_1 = q_{10}$) and plotting q_2 vs. p_2 for $\dot{q}_1 \geqslant 0$ (p_1 is then fixed by energy conservation); this is a cross section of the energy shell. Similarly,

the quantal surface of section (QSOS) is given by the Husimi function with similarly chosen values of the variables:

$$S_{q_1=q_{10}}(q_2, p_2, E) = \mathscr{H}[q_1 = q_{10}, q_2, p_1(E, q_{10}, q_2, p_2), p_2] \tag{8}$$

Surfaces of section are useful as a diagnostics for the degree of chaos in the classical system. Tori will appear as smooth, closed curves. However, if the classical limit is not integrable, phase space will not be completely foliated by tori, and there will be regions of chaos represented as a sea of dots (see Fig. 1a).

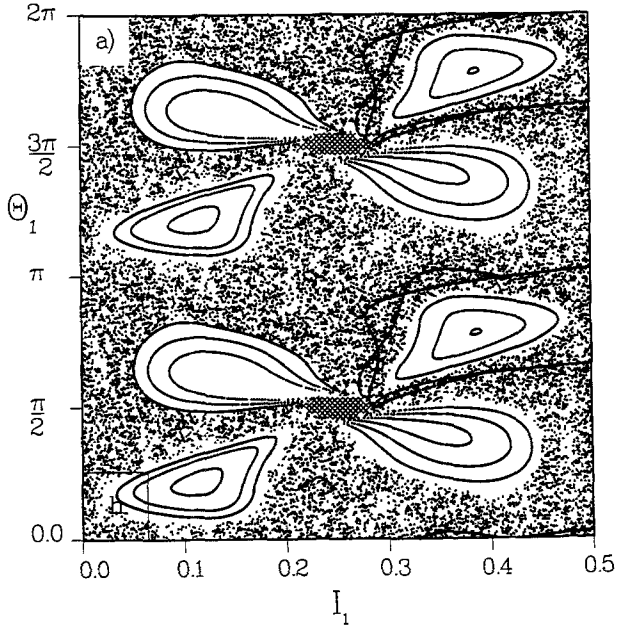

(a)

Fig. 1. (a) A classical surface of section at $I_2 = 0.5$ for the Hamiltonian (31) at $E = -0.09$. The crosses indicate energetically inaccessible regions. The smooth curves enclosing a white area are KAM tori; each is made by one trajectory. These are the regular regions of phase space. The sea of dots was made by a single trajectory in the chaotic region. The remaining smooth lines within the chaotic sea are the stable and unstable manifolds of the unstable periodic trajectory. Note that the periodic trajectory $I_0 = 0$ is the entire $I_1 = 0.5$ line. (b) The QSOS (8) for a state associated with a KAM torus. (c) The same for a state associated with the $I_0 = 0$ periodic orbit; the eigenvalue is very close to an energy that quantized the action of that orbit. The circles are the stable and unstable manifolds of that orbit. (d) A state scarred by both the $I_0 = 0$ and $I_1 = I_0$ periodic orbits. The SUM for the $I_0 = 0$ orbit is shown with circles; the SUM for the $I_1 = I_2$ orbit is shown with crosses. This state is far from an energy which quantizes the $I_0 = 0$ orbit. (e) An eigenstate scarred by the $I_1 = I_0$ periodic orbit and the stable and unstable manifolds of that orbit. (f) The only state in the energy region that is close to ergodic.

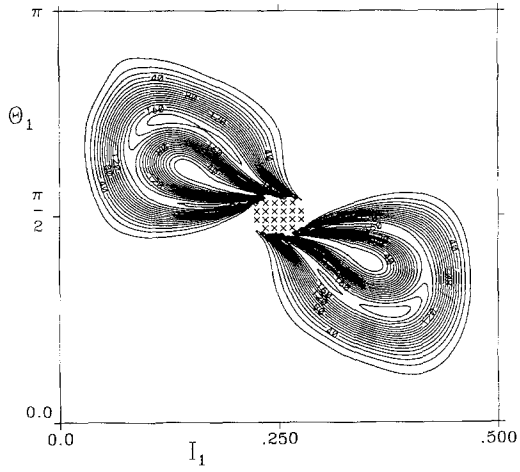

(b)

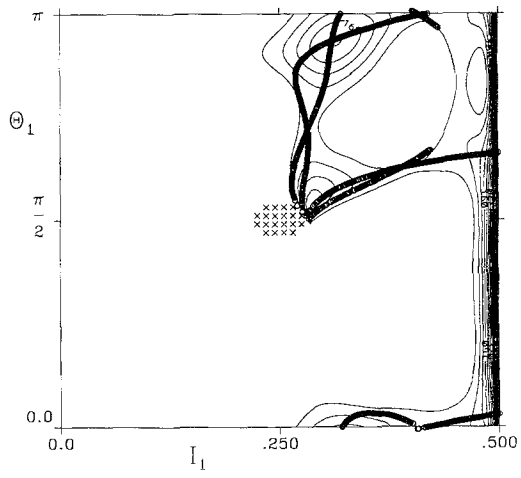

(c)

Fig. 1. (*Continued*)

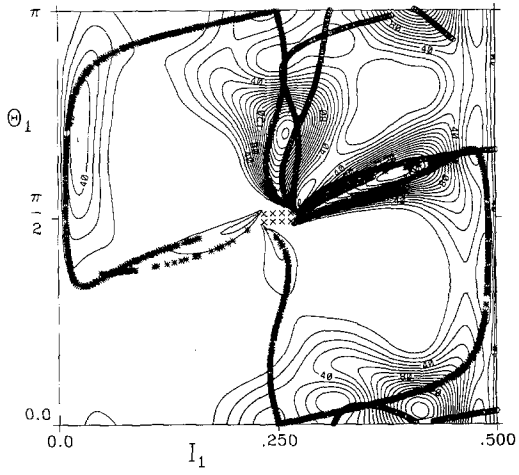

(d)

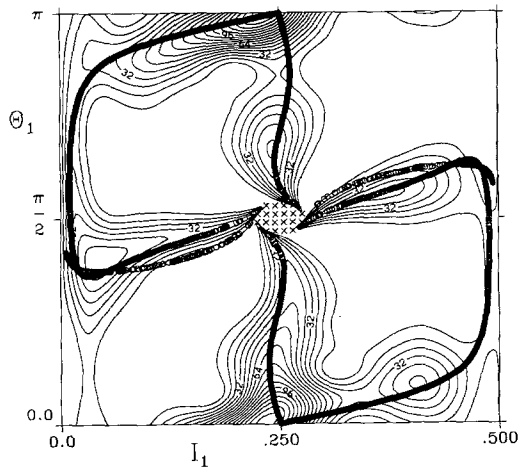

(e)

Fig. 1. (*Continued*)

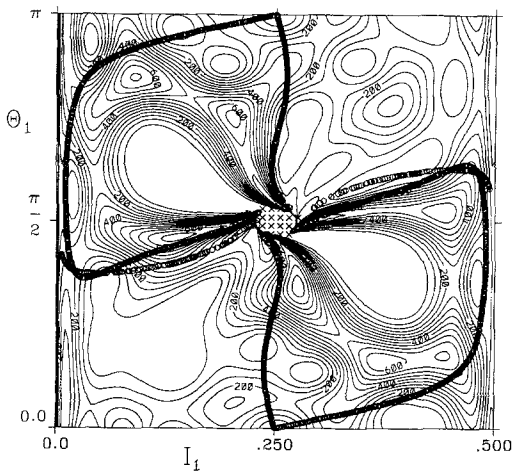

(f)

Fig. 1. (*Continued*)

3. SEMICLASSICAL WAVEFUNCTIONS FOR NONINTEGRABLE SYSTEMS

We now have the energy eigenstates for integrable systems in both phase space (6) and coordinate space (2), but integrable systems are not typical. Typical systems have regular regions populated by KAM tori (those tori that persist even though the system is nonintegrable) and chaotic regions where tori no longer exist.[7] EBK quantization cannot be extended to these systems without tori. However, we can attempt to generalize what we have learned about Wigner functions: they should be localized on the regions of phase space covered by a typical trajectory. In particular, for ergodic systems (those with no tori left), a typical trajectory covers the entire shell, so the corresponding Wigner function would be as follows:

$$W_\psi(\mathbf{q}, \mathbf{p}) = \frac{\delta[E - H(\mathbf{q}, \mathbf{p})]}{\int d\mathbf{q}'\, d\mathbf{p}'\, \delta[E - H(\mathbf{q}', \mathbf{p}')]} \tag{9}$$

This was in fact an early, independent conjecture of Berry and Voros.[19]

Recalling that $|\Psi(\mathbf{q})|^2$ is the projection of the Wigner function onto coordinate space, we can therefore also say something about the probabilities. For example, if the Hamiltonian is two-dimensional and of the form $(p_1^2 + p_2^2)/2m + V(q_1, q_2)$, then (9) implies a constant probability over the energetically allowed region of coordinate space. However, this

result cannot be correct since the probabilities must oscillate in the classically allowed region. Instead, we must interpret (9) as the correct result when we average over small regions in phase space, and the resulting probability (obtained by projecting down onto coordinate space) as a smoothed wavefunction. In the semiclassical limit, we can average over many wavelengths, yet take the averaging interval to zero, indicating that Ψ can have large variations in the probability amplitude and yet be agreement with Eq. (9).

This expectation of relatively smooth probabilities is essential because, as Heller points out,[20] a state can be considered localized only if it is less spread out than we would expect given prior constraints (e.g., energy conservation). Their conjecture gives us the context in which scars are so surprising.

This conjecture (9) for ergodic systems was supported by the independent works of Shnirelman, Zelditch, and Colin de Verdiere.[21] They looked at ergodic geodesic flow, and found that the eigenstates of the Laplacian (the free Hamiltonian) obey the following relation:

$$\lim_{j\to\infty} \int_{\mathcal{M}} d\mathbf{q}\, a(\mathbf{q})\, |\Psi_j(\mathbf{q})|^2 = \frac{\int_{\mathcal{M}} d\mathbf{q}\, a(\mathbf{q})}{\int_{\mathcal{M}} d\mathbf{q}} \tag{10}$$

for smooth $a(\mathbf{q})$ and almost all j. That is, $|\Psi_j(\mathbf{q})|^2$ is essentially evenly spread over coordinate space, since as $j\to\infty$, the oscillations are so rapid that only the average value is picked up by the smooth function $a(\mathbf{q})$. Note that in this special case, the average value of the probability is a constant because there is no potential.

4. SCARRED WAVEFUNCTIONS

The earliest work done on the eigenfunctions of chaotic systems was by McDonald and Kaufman.[22] They worked in the stadium billiard—one of the few classical systems that is known to be ergodic. Many of their plots of Ψ_n gave the strong impression of stochasticity, just as was expected from semiclassical arguments. Yet they also found that some of the eigenstates did not have a probability amplitude evenly spread over the available coordinate space, but localized on short periodic orbits. This phenomenon was left as "an enigma" in their work.

Heller,[4] working in the same system, found the same phenomenon, explained the association with periodic orbits, and dubbed the behavior "scarring." His explanation is based on a time-dependent picture. If we launch a wave packet on an unstable periodic orbit (i.e., one whose

neighboring orbits are diverging exponentially), propagate it semiclassically, and plot the autocorrelation $\langle \Psi(t) \mid \Psi(0) \rangle$ of the wave packet, we see three time scales. Very quickly the autocorrelation drops to zero as the packet moves away from its initial position ($\Delta t \sim 1/\sigma$), then there is a recurrence at the period of the orbit ($\Delta t = \tau$), but there is also an exponential decay of the recurrence height ($\Delta t \sim 1/\lambda$) because the wave packet is falling off the unstable orbit. The rate of divergence, λ is the Lyapunov exponent of the orbit. If we Fourier transform the autocorrelation function, we obtain the power spectrum with energy scales inverse of those in time. The initial short dropoff in time gives rise to a wide (statistical) envelope in energy ($\Delta E \sim \sigma$). The recurrence at the period gives rise to oscillations about the envelope ($\Delta E \sim 1/\tau$), and the instability λ gives the width of those peaks ($\Delta E \sim \lambda$).

What does this say about the spread of the eigenfunctions in coordinate space? Those eigenstates that have larger than statistical overlaps with the initial wave packet will also have large overlaps with the wave packet for all time, and so have larger than statistical overlaps with the periodic orbit that the wave packet follows. This larger than statistical overlap is a scar on the wave function; the name arises because of the appearance of the contour plots of $\Psi_n(\mathbf{q})$; the large probability appears as a dense and dark set of contours (see Fig. 4). It is important to note that from the discussion of the autocorrelation function, if the product $\lambda\tau$ is large (i.e., the orbit is very unstable), then the autocorrelation function looks again like the broad statistical distribution, and no scarring occurs.

Heller has shown that this localization due to unstable periodic orbits is a specific case of a more general phenomenon: localization of eigenstates will occur whenever there are recurrences in the classical dynamics before the break time.[20] The break time is given by $\tau_B = hD(E)$, where $D(E)$ is the density of states; it is the time at which the dynamics notices the discreteness of the spectrum and after which not much new can happen in the quantum dynamics.

But $|\Psi(\mathbf{q})|^2$ may not tell us unambiguously which periodic orbit is responsible for the scarring, since periodic orbits can overlap in coordinate space. A less ambiguous identification can be made by looking in phase space. This was done first by Waterland *et al.*,[23] who examined the QSOS (8) for eigenstates of a chaotic quartic potential. Their results were convincing: they saw the Husimi distributions that were concentrated directly on the stable and unstable manifold (SUM) of the unstable periodic orbit. These are the manifolds that are created by propagating a swarm of initial conditions close to the periodic orbit both forward in time (for the unstable manifold) and backward in time (for the stable manifold) (see Fig. 1a). The energy-averaged Husimi functions were also concentrated

on the same manifolds. They noted that the scarring occurred near, but not predictably on, energies that quantized the action of the periodic orbit. Feingold *et al.*[24] have found that the association with the stable and unstable manifolds is clearer for the Wigner distribution than the Husimi, yet the detailed structure of the Wigner obscures all but the strongest scarring.

5. PERIODIC ORBIT THEORY AND SCARS

Our understanding of scarred states became more quantitative and detailed with the theoretical work of Bogomolny[25] and Berry.[26] Both started with the work of Gutzwiller[2] and Balian and Bloch,[3] which derived a semiclassical expression for the density of states in terms of a sum over periodic orbits of the classical system. This is a powerful and surprising formula, so we will take a detour in order to understand its origins.

The beginning point of this and the related calculations is the energy Green's function $G(\mathbf{q}, \mathbf{q}', E)$ which tells us all there is to know about the quantum system. For example, we can write the density of states as follows:

$$\begin{aligned}\rho(E) &= \sum_n \delta(E - E_n) \\ &= \frac{1}{\pi} \lim_{\varepsilon \to 0} \operatorname{Im} \int d\mathbf{q} \sum_n \frac{\Psi_n^*(\mathbf{q})\, \Psi_n(\mathbf{q})}{(E - E_n) + i\varepsilon} \\ &= \frac{1}{\pi} \lim_{\varepsilon \to 0} \operatorname{Im} \int d\mathbf{q}\, G(\mathbf{q}, \mathbf{q}, E + i\varepsilon) \end{aligned} \tag{11}$$

The other ingredient that we need is that the Green's function is the time Fourier transform of the propagator $K(\mathbf{q}, \mathbf{q}', t)$, which can be expressed as a Feynman path integral

$$K(\mathbf{q}, \mathbf{q}', t) = \int_{\text{all paths}} \mathscr{D}[\mathbf{q}(\tau)] \exp[iR(\mathbf{q}, \mathbf{q}', t)/\hbar] \tag{12}$$

where

$$\begin{aligned} R(\mathbf{q}, \mathbf{q}', t) &= \int_0^t \mathscr{L}(\mathbf{q}''(\tau), \dot{\mathbf{q}}''(\tau), \tau)\, d\tau \\ &= \int_{\mathbf{q}}^{\mathbf{q}'} \mathbf{p}(\mathbf{q}'') \cdot d\mathbf{q}'' - \int_0^t H(\mathbf{q}''(\tau), \mathbf{p}(\mathbf{q}''(\tau)), \tau)\, d\tau \end{aligned} \tag{13}$$

is Hamilton's principle function, $\mathscr{L}$ is the Lagrangian, and we integrate over all geometric paths (parametrized by τ) that go from $\mathbf{q}'$ to $\mathbf{q}$ in time t. Putting this all together, we have

$$\rho(E) = \lim_{\varepsilon \to 0} \operatorname{Im} \frac{1}{i\pi\hbar} \int d\mathbf{q} \int_0^t dt \int_{\text{all paths}} \mathscr{D}[\mathbf{q}(\tau)] \times \exp \frac{i[R(\mathbf{q}, \mathbf{q}', t) + (E + i\varepsilon)t]}{\hbar} \Bigg|_{\mathbf{q}=\mathbf{q}'} \tag{14}$$

The evaluation of $\rho(E)$ therefore requires three integrations; in the semiclassical limit, these can all be done by the stationary phase approximation (SPA). Each of the SPAs serves to limit the paths in the sum. We begin with all geometric paths in the Feynman path integral; evaluation of the path integral limits us to paths which obey classical dynamics:

$$\delta R(\mathbf{q}, \mathbf{q}', t) = 0 \tag{15}$$

since the stationary phase requirement is equivalent to Hamilton's principle. The resulting semiclassical formulation for $K(\mathbf{q}, \mathbf{q}', t)$ is known as the Van Vleck propagator.[10] (For a detailed derivation, see the monograph by Shulman.[30]) Next, the time integral limits the classical paths to those of energy E:

$$\frac{\partial(Et + R)}{\partial t} = E - H(\mathbf{q}, \mathbf{p}, t) = 0 \tag{16}$$

This equality also reduces the phase to the action

$$S(\mathbf{q}, \mathbf{q}') = \int_{\mathbf{q}}^{\mathbf{q}'} \mathbf{p} \cdot d\mathbf{q}'' \tag{17}$$

Lastly, the integral over space limits us to periodic orbits:

$$0 = \frac{\partial S}{\partial q_i}\Bigg|_{\mathbf{q}=\mathbf{q}'} = \frac{\partial S}{\partial q_i} + \frac{\partial S}{\partial q_j'}\frac{\partial q_j'}{\partial q_i}\Bigg|_{\mathbf{q}=\mathbf{q}'} = p_i(q_i) - p_i(q_i')\Big|_{\mathbf{q}=\mathbf{q}'} = 0 \tag{18}$$

and when we take the trace ($\mathbf{q} = \mathbf{q}'$), this says the initial and final momenta are equal, i.e., the trajectory is a periodic orbit.

This quick look at the SPA evaluation of the integral shows how we

come to consider only periodic orbits. The final expression, however, also requires a nontrivial evaluation of the amplitude and a more complete discussion of Maslov index,[2,31] which is too detailed to repeat here. The result is as follows:

$$\rho_{sc}(E) = \rho_0(E) + \rho_{osc}(E) \tag{19}$$

where

$$\rho_0(E) = \frac{1}{(2\pi\hbar)^N} \int \delta[E - H(\mathbf{p}, \mathbf{q})]\, d\mathbf{p}\, d\mathbf{q} \tag{20}$$

is the Thomas–Fermi term [which simply counts the area in phase space in units of $(2\pi\hbar)^N$ at the correct energy] which comes from orbits of zero length, and

$$\rho_{osc}(E) = \sum_{\substack{\text{periodic} \\ \text{orbits } p}} \sum_{n} A_p \cos[nS_p(E)/\hbar - in\mu_p \pi/2] \tag{21}$$

where $S_p(E)$ is the action (17) of the pth orbit, and n is the number of traversals of the primitive (one time around) periodic orbit. The Maslov index μ_p essentially counts the number of times that the amplitude diverges, and the amplitude itself (A_p) contains information about the stability and period of the orbit. In particular, for an unstable fixed point, we have

$$A_p = \frac{T_p}{\pi\hbar \sinh(n\lambda_p/2)}$$

where T_p is the period of the primitive periodic orbit; λ_p is the Lyapunov exponent.[67] This trace formula has been extended to systems with continuous symmetries by Creagh and Littlejohn.[32]

Equations (11) and (21) say that the eigenvalues can be obtained semiclassically by looking for the values at which the periodic orbit sum diverges. Note that periodic orbit quantization, unlike Bohr–Sommerfeld, works for any classical system, whether or not tori exist. Also, Berry and Tabor[27] showed that for an integrable system, the two quantization methods are equivalent. This can be seen as follows: if we are near a quantized torus, there is a series of nearby resonant tori (i.e., ones with commensurate frequencies and therefore periodic orbits) the ratio of whose frequencies are rational approximates of the ratio of frequencies on the quantized torus. Under certain conditions,[39] phases of the periodic orbit and all of its repetitions add coherently to the sum, and give a divergent contribution to the density of states.

However, formula (21) is not without difficulties. It says that we must sum over all periodic orbits, yet the number of periodic orbits grows exponentially with the period τ. Does this sum converge at all, and does it converge at real values of the energy? Gutzwiller[28] was able to do the sum for the anisotropic Kepler problem. This tour de force was possible because there exists a binary coding for the periodic orbits, and the action can be approximated in terms of that code. The resulting semiclassical eigenvalues of low-lying states were in good agreement with the quantum mechanical calculations, and the imaginary parts of the energy were small. For the hydrogen atom in a magnetic field, where the entire sum cannot be done, Wintgen[29] summed (21) over 13 orbits with the smallest action, and found that these give good results for the few lowest eigenvalues. Recently, much effort has been put into the method of cycle expansion for speeding up convergence and making this a computationally tractable method for quantization.[33]

A surprising source of help in the understanding of the analytical properties of (21) are the zeros of the Riemann zeta function

$$\zeta(s) = \sum_{n=1}^{\infty} \frac{1}{n^s} = 0 \tag{22}$$

which are hypothesized to lie on the line $\mathrm{Re}(s) = 1/2$. The zeros do not come from a dynamical system (as far as we know), but the oscillating part of their density along the line $\mathrm{Re}(s) = 1/2$ gives a form exactly like that of (21) if we identify the dynamical functions (e.g., action and Lyapunov exponent) with functions of the prime numbers. The analytic framework supplied by the zeta function (the functional equation, in particular) has been used by Berry and Keating[34] to study the convergence properties of the trace formula. Sieber and Steiner[35] have used the dynamical zeta function and the trace formula to quantize the hyperbola billiard, and Tanner *et al.*[36] combine the cycle expansion and functional equation to obtain reliably and efficiently eigenvalues for the anisotropic Kepler problem and three-disk billiard system.

Lastly, there have always been doubts about the long-time accuracy of the Van Vleck propagator. Recent work by Tomsovic and Heller[37] has shown that the semiclassical propagator and the exact quantum dynamics give autocorrelations $\langle \Psi(0) \mid \Psi(t) \rangle$ for Gaussian wave packets in the stadium billiard which agree in great detail for times ($t = 6$) much longer than the break time ($t \approx 2$). Even though the classical swarm of initial conditions has become long and filamentary by $t = 6$ (the swarm has folded over at least 30,000 times), this classical dynamics in the semiclassical theory accurately represents the quantum dynamics. They conclude that

"the intricate dynamics of chaotic motion do not have the strong adverse effect on the fundamental semiclassical approximation that had been believed." This work gives renewed hope that semiclassical procedures can succeed even though the classical and quantum dynamics bear little resemblance to one another.

Returning to our main theme of wavefunctions, Berry and Bogomolny used the same ideas to calculate their scar formulas: beginning with the semiclassical propagator and evaluating integrals via SPA. Bogomolny used the following relation for the probability in coordinate space:

$$|\Psi(\mathbf{q})|^2 = \frac{\operatorname{Im} G(\mathbf{q}, \mathbf{q}, E)}{\int d\mathbf{q}' \operatorname{Im} G(\mathbf{q}', \mathbf{q}', E)} \tag{23}$$

To evaluate this semiclassically, he followed the above procedure for the density of states, but did not take the final integral over $\mathbf{q}$. This implies that his sum included all classical orbits at energy E, not just the periodic ones. However, by averaging over small regions in $\mathbf{q}$ and short energy intervals, he limited the sum to closed orbits near short periodic orbits (i.e., $\mathbf{q} = \mathbf{q}'$ and $\mathbf{p} - \mathbf{p}'$ small). The resulting formula for the probability (averaged over both space and energy) has a smooth term which is the space and energy average of (9). The oscillatory term gives a detailed picture of the contribution from trajectories in the neighborhood of single periodic orbit. Qualitatively, the strength of the scar is $[\hbar/m_{12}(x)]^{1/2}/|\dot{q}|$ and the width is $\hbar^{1/2}/W(x)$, where $m_{ij}(x)$ is an element of the monodromy matrix,[31] $W(x) = [(m_{11}(x) + m_{22}(x) - 2)/m_{12}(x)]$, and $|\dot{q}|$ is the modulus of the velocity. Also, he showed that the probability maximum is sometimes on the orbit itself, and sometimes symmetrically just off the orbit, and that the probability is greatly enhanced at self-focal points where $m_{12}(x)$ is zero.

Berry, on the other hand, chose to look at the Wigner function by taking the Weyl transform of the Lorentzian-smoothed spectral operator:

$$\delta_\varepsilon(E - \hat{H}) \equiv \frac{1}{\pi} \operatorname{Im} \frac{1}{(E + i\varepsilon - \hat{H})} \tag{24}$$

which is equivalent to energy-smoothed Wigner functions of the energy eigenstates:

$$\begin{aligned} W(\mathbf{q}, \mathbf{p}, E, \varepsilon) &= (2\pi\hbar)^N \sum_n \delta_\varepsilon(E - E_n)\, W_{\psi_n}(\mathbf{q}, \mathbf{p}) \\ &= \int d\mathbf{q}'\, e^{i\mathbf{p}\cdot\mathbf{q}'} \left\langle \mathbf{q} + \frac{\mathbf{q}'}{2} \middle| \delta_\varepsilon(E - \hat{H}) \middle| \mathbf{q} - \frac{\mathbf{q}'}{2} \right\rangle \\ &= \frac{2}{\hbar} \operatorname{Re} \int d\mathbf{q}'\, e^{i\mathbf{p}\cdot\mathbf{q}'} \int_0^\infty dt\, e^{[iE - \varepsilon]t/\hbar} K\left(\mathbf{q} - \frac{\mathbf{q}'}{2}, \mathbf{q} + \frac{\mathbf{q}'}{2}, t\right) \end{aligned} \tag{25}$$

The evaluation of this integral again involves three SPA, but with slightly different results than before. This time, because of the spatial arguments of the propagator, we find that the SPA evaluation of $K(\mathbf{q}-\mathbf{q}'/2, \mathbf{q}+\mathbf{q}'/2, t)$ limits the paths to classical paths beginning at $\mathbf{q}_A \equiv \mathbf{q}-\mathbf{q}'/2$ and ending at $\mathbf{q}_B \equiv \mathbf{q}+\mathbf{q}'/2$. Together, these give the midpoint rule:

$$\mathbf{q} = \frac{\mathbf{q}_A + \mathbf{q}_B}{2} \tag{26}$$

i.e., the only paths that contribute to $W(\mathbf{q}, \mathbf{p}, E, \varepsilon)$ are those whose initial and final points define a chord whose midpoint is $\mathbf{q}$. The spatial integral then limits the sum to paths for which

$$\mathbf{p} = \frac{\mathbf{p}_A + \mathbf{p}_B}{2}$$

The time integral limits the sum to those with energy E, and also to periodic orbits ($\mathbf{q}_A = \mathbf{q}_B$; $\mathbf{p}_A = \mathbf{p}_B$), since for these orbits both the first and second derivatives of the phase are zero. Hence in this phase space picture, the relation to periodic orbits falls out, and is not the result of averaging. The final result again has a smooth part, which is just the energy-smoothed version of (9). The oscillatory contribution from one periodic orbit is the main result of Berry's work, but is too detailed to reproduce here. Qualitatively, this contribution is an Airy function as we move off of the energy shell, and sinusoidal oscillations of constant amplitude as we move off the periodic orbit but stay on the energy shell.

This work was extended to billiard systems by Feingold *et al.*[24] In these systems the formula must be modified since one term (containing the first and second time derivatives of the momentum) disappears. The result is that scars are deeper in the semiclassical limit for billiards [$W \sim \mathcal{O}(\hbar^{-1})$] than for smooth potentials [$W \sim \mathcal{O}(\hbar^{-2/3})$].

In both of these works, we are given explicit details of the contribution of one periodic orbit to a wavefunction. However, it is known that a single orbit cannot support a state. (Recall that for integrable systems it was the whole family of periodic orbits that gave rise to a state.) Yet some states seem to be completely localized on one single periodic orbit. Ozorio de Almeida[39] addressed this question by examining the homoclinic torus (i.e., the Lagrangian torus made up of the central periodic orbit and the initial, smooth pieces of the stable and unstable manifolds). Inside each such torus is an infinity of long, periodic orbits that spend much of their time in the vicinity of the unstable central orbit. Therefore their actions can be simply related to the action of the central periodic orbit, and under certain

circumstances ($\lambda\tau \leqslant 2 \ln 2$ and the quantization of the action of the central periodic orbit), they can contribute coherently to make a divergent contribution to a state. This work explains why we would expect the scarred states to be localized along the SUM of the unstable periodic orbit.

6. CURRENT WORK

There are many questions that are still unresolved concerning scars. The formulas of Berry and Bogomolny describe energy-averaged functions, not individual states, and give the contribution from one periodic orbit. Any individual state has contributions from all periodic orbits. Some questions that have been investigated include the following: Are individual wavefunctions clearly scarred, or only energy averages? At what energies do scarred wavefunctions appear? How is the scarring strength shared between wavefunctions? How large can $\lambda\tau$ be before scarring disappears? Are there any truly ergodic wavefunctions? How does scarring scale with $\hbar$? In an effort to answer these and other questions, there has been much numerical and analytical work done on scars in a wide variety of systems. What follows is at best a partial list of contributors.

To the best of our knowledge, scarred eigenfunctions exist in all nonintegrable systems (at least all systems where anyone has looked), even though the classical dynamics of these systems covers the range from pseudointegrable to hard chaos. The least chaotic systems are pseudointegrable billiards; these are billiards that have constants of the motion which are in involution everywhere except at the vertices. As a result, the phase space is foliated by tori with two or more handles. Although the phase space is quite ordered, there is no way to find action–angle variables, and EBK quantization fails. Biswas and Jain[44] and Šeba and Zyczkowski[45] have been scarring in such billiards.

On the other end of the dynamical spectrum, scars have been seen in systems with hard chaos. Saraceno and Ozorio de Almeida[46] [based on work of Balazs and Voros[47]] have worked with the quantized Baker's map, which is known to have no stable periodic orbits and exponential divergence of trajectories, and therefore exhibits hard chaos. In this system, the simplicity of the classical map allows a detailed analysis of the eigenstates in terms of classical structures. They are able to see that whole families of periodic orbits are necessary to support the eigenfunctions. Aurich and Steiner[48] studied a free particle moving on a compact Riemann surface of constant negative curvature, which is also known to exhibit hard chaos. These surfaces of constant negative curvature are of great interest in periodic orbit theory, since the density-of-states formula (21) is exact for these systems, and not a semiclassical approximation. The

authors were therefore able to derive an exact sum rule for the eigenstates and also found that it is not a single orbit, but a whole collection of periodic orbits that contribute to scarring.

Scarring is also not confined to time-independent systems: this phenomenon has been seen in the quasienergy eigenfunctions of a kicked rotor by Kuś *et al.*[49] and by Jensen *et al.*[50] in eigenstates of hydrogen in a microwave field.

Researchers have begun to investigate Bogomolny's formula in specific systems. Scarred wavefunctions of a hydrogen atom in a magnetic field have been quantitatively investigated by Wintgen and Hönig[38] and Delande.[51] In particular, energy-averaged scar measures are shown to peak at quantized values of the action, details of the shape of wavefunctions are well-described by Bogomolny's work, and the $\hbar$ dependence of the width and strength of the scar (both go as $\hbar^{1/2}$) are in agreement with theory. On the other hand, Frisk[52] looks at eigenstates of a family of billiards and finds that scarring strength is underestimated by this theory, and that the decrease in scarring strength is correlated to the Kolmogorov–Sinai entropy (a global measure of the degree of chaos), and not the stability of the individual orbits. Frisk also finds that scars persist even when $\lambda\tau = 10$ for the periodic orbit that scars the wavefunction.

There has been some success in predicting which states will be scarred. Investigations of the quartic oscillator by Eckhardt *et al.*[53] and the $\pi/3$ rhombus billiard by Biswas and Jain[44] use adiabatic breakup[54] to predict the energies at which periodic orbits will scar wavefunctions. This method works well in the systems studied, but it is not without practical difficulties (e.g., the appropriate choice of coordinates is essential but nontrivial) and limitations (e.g., it only works for periodic orbits that come in bands).

Several researchers have investigated scarred wavefunctions in conjunction with measures of randomness. Berry conjectured[5] that for ergodic systems, the wavefunctions would be superpositions of infinitely many deBroglie waves with all possible directions (since the classical particles can have all possible directions). Then the wavefunction should be Gaussian random and the correlations should be isotropic. McDonald and Kaufman[55] have studied eigenstates in the stadium billiards and find that although typical states are described by Gaussian random statistics, they are not evenly spread over the available configuration space (even if they allow for smoothing over several wavelengths) and conclude that they are not evenly spread over the energy shell in phase space. Localized states, on the other hand, deviate greatly from Gaussian random behavior.

Very similar results are found by Biswas and Jain[44] in the $\pi/3$ rhombus billiards, and Šeba and Zyczkowski[45] in the Sinai billiard with a point scatterer, even though the classical dynamics of the systems is very

different (hard chaos vs. pseudointegrability). In particular, they find that many states show Gaussian random behavior (though not the localized ones). However, the correlation functions for these Gaussian random states deviate from expectation for large spatial separations, indicating that there are not a large number of plane waves in these eigenfunctions. The Gaussian random behavior in these systems can be understood by noting that as few as six superimposed plane waves with random directions (one from each branch of these somewhat more complicated tori) are enough to create random wavefunctions.[56] The conclusion is that Gaussian randomness is a necessary but not sufficient criterion for chaos in the classical limit.

Biswas *et al.*[40] have made a connection between the results of periodic orbit theory (POT) and random matrix theory (RMT) (which has also played a large role in quantum chaology; for a general review of RMT see ref. 41; for a review of RMT and quantum chaology see ref. 42). They argue heuristically that the contributions from each periodic orbit and its nearby closed orbits contribute to an energy eigenstate as independent random variables with zero average and finite width so that the amplitude of the eigenfunction has a Gaussian distribution. This is exactly the distribution expected if the Hamiltonian is a typical member of the Gaussian orthogonal ensemble of random matrices, as conjectured by Bohigas *et al.*[43]

Heller and co-workers have investigated very general questions about scars. O'Connor and Heller[57] have studied the $\hbar$ dependence of scarring in the stadium billiard. They argue that scarred states are a set of measure zero as the classical limit is approached (although they are infinite in number), so that there is no conflict between localization of these states and the correspondence principle as expressed in the work of Shnirelman, Zelditch, and Colin de Verdiere.[21] Heller *et al.*[58] show that random superpositions of plane waves obeying discrete symmetries can be localized even when there are no underlying periodic orbits, cautioning us against quick scar evaluations. They also discuss ways in which the order of scars and the original notion of random wavefunctions can be compatible.

Finally, it is important to note that scarring and its effects have been seen in experiment. Sridhar[59] has done experiments in microwave cavities shaped liked the chaotic Sinai billiard and found that some of the modes are indeed localized on unstable periodic orbits. In experiments ionizing Rydberg hydrogen atoms in microwave fields, certain energy states were found to be more stable against ionization than their neighbors. Jensen *et al.*[50] have been able to explain this stability by noting that the corresponding quasienergy eigenfunction is localized in phase space so the atom has little probability to ionize. They present this localization as a new method for the quantum inhibition to transport.

7. MODEL HAMILTONIAN

The model that we study is unusual in that the classical Hamiltonian is not kinetic plus potential, and the phase space is compact. Yet here, too, scarring is clearly present.

The model is a schematic shell model, with its origins in nuclear structure physics.[60] It represents N interacting fermions that are allowed to occupy three different single particle levels or shells. Each shell is N-fold degenerate, so there is no Pauli blocking. The Hamiltonian has two terms: the first is a single-particle Hamiltonian and the second is a simplified two-body interaction.

This Hamiltonian can be written in terms of the generators G_{ij} of a $U(3)$ algebra,[61]

$$H = \sum_{i=0}^{2} \varepsilon_i G_{ii} + \frac{V}{2} \sum_{i \neq j = 0}^{2} G_{ij}^2 \tag{28}$$

where

$$G_{ij} = \sum_{m=1}^{N} a_{im}^{+} a_{jm}; \qquad G_{ij}^{+} = G_{ji}; \qquad i, j = 0, 1, 2 \tag{29}$$

and (a_{im}^{+}, a_{im}) are the usual creation–annihilation fermionic operators. Due to the conservation of the total number of particles, these operators are subject to the additional constraint $G_{00} + G_{11} + G_{22} = N$, and therefore the dynamical symmetry is now reduced to an $SU(3)$ algebra.

In (28) the labels i and $j = 0$, 1, or 2, and indicate the ground, first, or second single-particle level. The energy of each level is given by ε_i, and the interaction strength is given by V. We solve this Hamiltonian in the basis which is completely symmetric under interchange of particle labels. The basis states are labeled by $|n_1, n_2\rangle$, where n_i is the number of particles in level i.

Although the quantum problem is straightforward to solve, one cannot obtain the classical limit in the standard way—there is no $\hbar$ to take to zero. However, as $N \to \infty$, the system becomes macroscopic and should behave classically. It has been shown that the $N \to \infty$ limit does play the role of $\hbar \to 0$.[16] Coherent states play a key role in this limit: classical limits of physical observables are the expectation values of corresponding quantum operators between normalized coherent states. As $N \to \infty$, the spread in the coherent state decreases and the state closely resembles a classical point. The coherent states and the $N \to \infty$ limit have been studied in detail for this model by Leboeuf and Saraceno.[62,63]

In the semiclassical limit, the interaction parameter V is properly scaled as $\chi \equiv (N-1)V/\varepsilon$. It was found[64] that for $\chi \geqslant 100$ there are large energy ranges for which the classical dynamics is chaotic. As we are mainly

interested in this regime and as the Hamiltonian simplifies considerably in the $\chi \to \infty$ limit, from now on we take the following rescaled Hamiltonian:

$$\chi = \infty; \qquad H \to H/(N\chi) \tag{30}$$

For this value of the coupling, the classical dynamics exists only for $-1/4 \leqslant E \leqslant 1/3$. In this range, only the very high and low energies are quasi-integrable (i.e., phase space has very small chaotic regions). Judging by the fraction of trajectories with positive Lyapunov exponents, the dynamics is mixed regular and chaotic for $-0.15 \leqslant E \leqslant 0.02$ and chaotic for $0.02 \leqslant E \leqslant 0.24$.

Also for this coupling, the classical Hamiltonian in terms of action–angle variables can be written as follows:

$$\begin{aligned} \mathscr{H}(\mathbf{I}, \theta) = {} & I_0 I_2 \cos 2(\theta_2 - \theta_0) + I_1 I_0 \cos 2(\theta_0 - \theta_1) \\ & + I_1 I_2 \cos 2(\theta_2 - \theta_1) \end{aligned} \tag{31}$$

where the action variables (I_0, I_1, I_2) are the classical continuous analogs of the shell occupation numbers (n_0, n_1, n_2) (scaled by N) and satisfy the conditions

$$0 \leqslant I_i \leqslant 1, \qquad i = 0, 1, 2 \tag{32}$$

$$I_0 + I_1 + I_2 = 1 \tag{33}$$

The Hamiltonian is N-independent due to the normalization (30). We have written (31) in terms of three degrees of freedom to display the symmetry of the classical motion upon interchange of the single-particle labels. However, (33) provides a second constant of the motion (besides the energy), which reduces the motion to two degrees of freedom. These can be chosen to be the populations of any two of the levels and the corresponding angle differences. In what follows we choose as variables I_1 and I_2, so that the Hamiltonian (31) is now written only in terms of the actions (I_1, I_2) and their conjugate angles (θ_1, θ_2). The corresponding action space is the isosceles triangle, given by (32) with $i = 1, 2$.

8. PERIODIC ORBITS AND SCARRING IN THIS MODEL

In order to study scars, we must identify the short, unstable periodic orbits. As was pointed out in ref. 63, the $SU(3)$ model has several simple families of periodic orbits lying on the invariant planes given by $I_i = 0$ or $I_j = I_k$; a quick examination of Hamilton's equations of motion reveals that these are indeed invariant. From number conservation (33), these con-

straints reduce the Hamiltonian to a one-degree-of-freedom problem for which all trajectories are periodic orbits.

In previous work[65] we focused on the $I_0 = 0$ periodic orbit. This orbit exists for $-0.25 \leqslant E \leqslant 0.25$, and is unstable for $-0.236 \leqslant E \leqslant 0.25$. The strength of the scarring was measured by taking the overlap of the eigenfunctions with the eigenstates of the number operator that lie along the $I_0 = 0$ line:

$$P_m = \sum_{n_1} |\langle n_1, N - n_1 \mid \psi_m \rangle|^2 \tag{34}$$

We found that this quantity, averaged over energy, behaves much as the results in Section 5 would predict. There is a smooth background which is well described by (9), integrated over the coordinates (the angles, in this case), and Lorentzian-smoothed in energy. On top of the smooth background, there are oscillations whose peaks are at values of E that quantize the action of the periodic orbit. In the following discussion, we will refer to the energy interval surrounding the peak as the scarring region, and the energy interval surrounding the trough as the antiscarring region. This scarring persisted even when the instability of the orbit ($\lambda\tau$) exceeds 20, but the strength of the scarring did decrease as the instability increased, as predicted by Bogomolny.[25]

Finally, in order to further establish the connection between the eigenstates and the periodic orbits, we examined the wavefunctions in phase space using the Husimi distribution and quantal surfaces of section. For this system, the coherent states in the symmetric number basis can be written

$$\begin{aligned} &\langle I_1, I_2, \theta_1, \theta_2 \mid n_1 n_2 \rangle \\ &\quad = \left[\frac{N!}{n_1!\, n_2!\, (N - n_1 - n_2)!} I_1^{n_1} I_2^{n_2} (1 - I_1 - I_2)^{N - n_1 - n_2} \right]^{1/2} \\ &\qquad \times \exp(i n_1 \theta_1) \exp(i n_2 \theta_2) \end{aligned} \tag{35}$$

i.e., a trinomial distribution centered on $I_i = n_i/N$. For both the quasichaotic region and the chaotic region, scarred states were localized on the stable and unstable manifolds; moreover, in the quasichaotic region they were maximum at homoclinic points, i.e., the points where the stable and unstable manifolds cross.

One suggestion of Heller[4] is that there may be no ergodic eigenstates in the sense of (9). We investigate this proposal first where the dynamics is relatively simple, yet interesting: the quasichaotic region. We looked at 40 states between $-0.098 \leqslant E \leqslant -0.082$; this energy range covers one

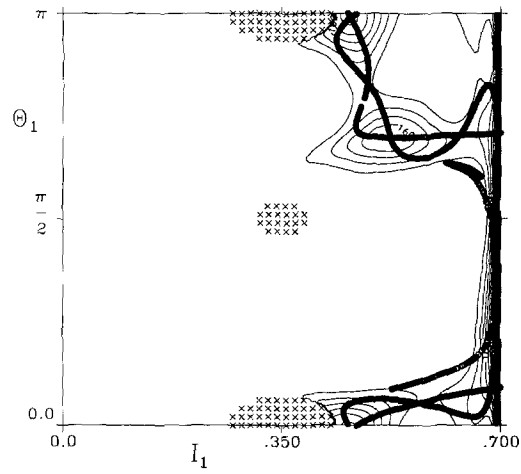

(a)

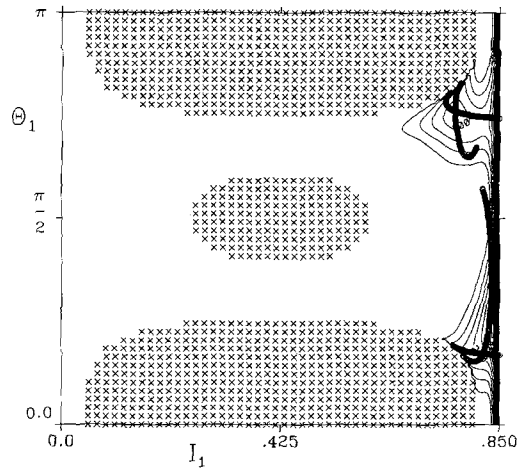

(b)

Fig. 2. (a) The same state and manifolds as in Fig. 1c, but on the $I_2 = 0.3$ surface of section. (b) The same as in Fig. 1c, but on the $I_2 = 0.15$ surface of section. Note that in both (a) and (b), the quantal surface of section remains a maximum on the homoclinic point. (c) The same state and manifolds as in Fig. 1d, but on the $I_2 = 0.3$ surface of section. (d) The same as in Fig. 1d, but on the $I_2 = 0.15$ surface of section. Note that the QSOS in all cases ($I_2 = 0.5$, 0.3, 0.15) is localized on both sets of manifolds.

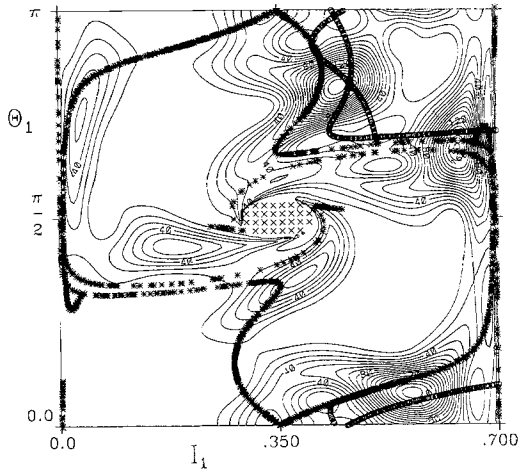

(c)

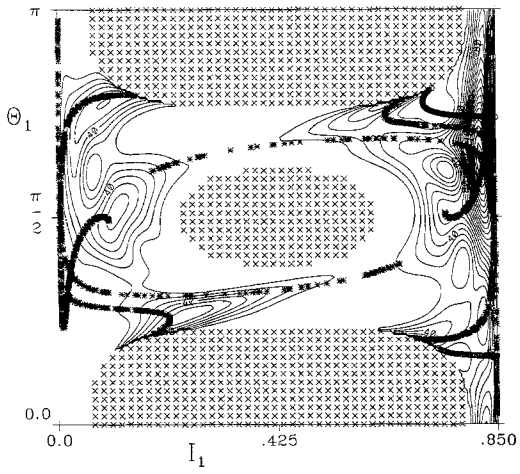

(d)

Fig. 2. (*Continued*)

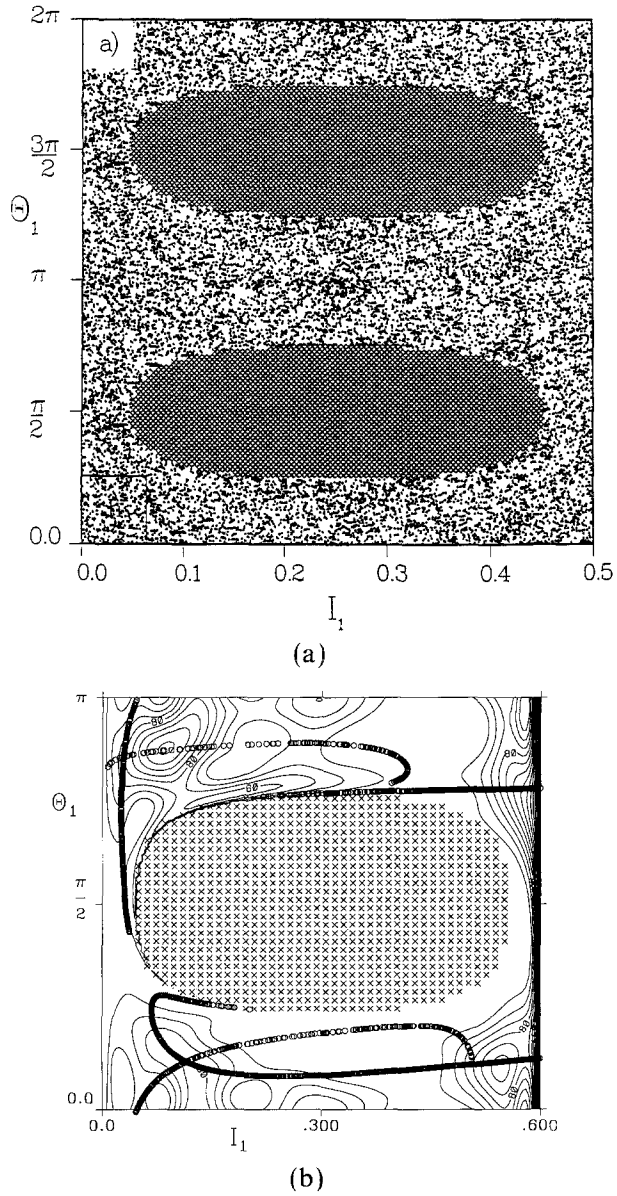

Fig. 3. (a) The classical surface of section for $I_2 = 0.5$ and $E = 0.1847$. The crosses indicate energetically inaccessible regions. Note that at this energy there are no visible regular regions left. (b) The quantal surface of section ($I_2 = 0.4$) for a state scarred by the $I_0 = 0$ orbit whose energy nearly quantizes the classical action. Recall that this periodic orbit is the entire $I_1 = 0.6$ line. (c) The same for a state scarred by the same orbit, but at an energy which does not quantize the action. (d) A state that is close to ergodic.

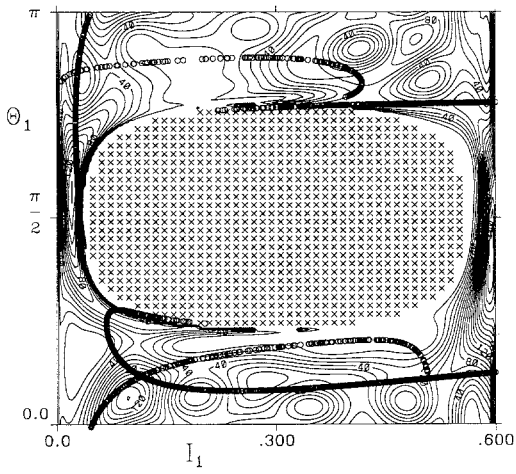

(c)

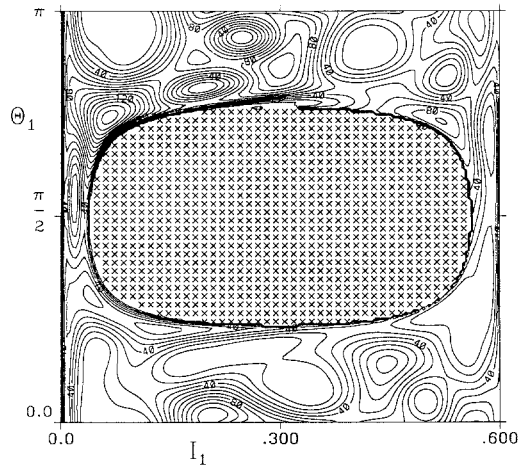

(d)

Fig. 3 (*continued*)

scarring and one antiscarring energy interval. Although the phase space is approximately 50% chaotic at this energy (see Fig. 1a), there was only one state in this set that was not readily identifiable as either an eigenstate associated with a torus (13 states), with an $I_i = 0$ periodic orbit (5 states), with an $I_i = I_j$ periodic orbit (10 states), or with a mixture of both periodic orbit families (11 states) (see Fig. 1). Therefore, although the chaotic region is large enough to support states, almost all states are localized on tori or on stable and unstable manifolds. In order to claim that these states are not ergodic, we must consider what would happen if we were to smear theses states over a region of size $2\pi\hbar$ (see the small box in Fig. 1a). For the states in Figs. 1b–1d we see that even such averaging would not give an even distribution. However, the state in Fig. 1f (after averaging) would be quite smooth in the ergodic region.

It is well established that we cannot predict which individual states will be scarred. Quantization of the action predicts the maximum in the energy-averaged scar measure, but not the energy of an individual scarred state. In fact, in our system the eigenvalues of some scarred states are within an antiscarring interval (see Fig. 1d). However, there is a qualitative difference between the scarred states in the scarring interval and those in an antiscarring interval. Those scarred states nearest in energy to the value which quantizes the action are completely localized on the SUM of the scarring orbit (Fig. 1c). However, those in the antiscarring interval are clearly supported by at least two periodic orbits (Fig. 1d). Therefore, while the quantization rule is of little help in predicting where scarring will occur, it does locate the regions of the most dramatic scarring.

In order to check that these associations with periodic orbits and their SUM are not coincidence or imagination, we looked at other quantal surfaces of section (i.e., $I_2 = 0.3, 0.15$). Figure 2 shows these for a scarred state in the scarring interval and for a scarred state in the antiscarring interval. For the state in the scarring interval, we can see that the association persists, including the maxima on the homoclinic points. For the state in the antiscarring interval, we see that all of the surfaces of section show the state localized around the SUM of both the $I_0 = 0$ and $I_1 = I_0$ orbits.

Motivated by the extreme order in the quasichaotic regime, we looked for order in the chaotic regime. Again we looked at a range of states that spanned a scarring and antiscarring interval ($0.175 \leqslant E \leqslant 0.195$). Here, of the 29 states, only 13 are easily associated with a particular manifold. The remaining states could be identified with multiple classical structures by careful inspection of both the action plots (Fig. 4) and the QSOS (Fig. 3). These two provided complementary information. The action plots gave the global picture of phase space, although some information is lost in the projection down onto action space. This lost information can be recovered

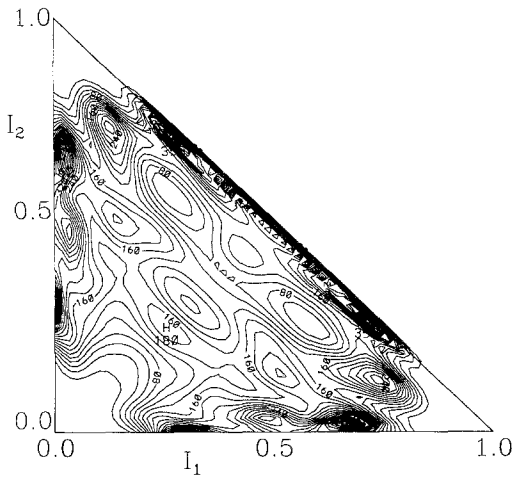

(a)

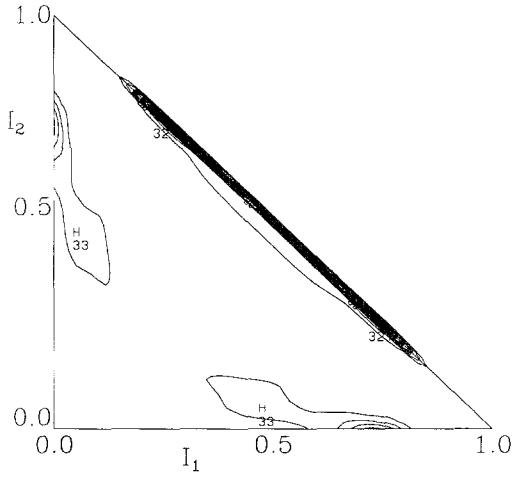

(b)

Fig. 4. (a) The Husimi distribution, projected onto action space for the state shown in Fig. 3d. Note that in action space the state does not appear ergodic, because it avoids the center. However, inspection of Fig. 3a shows that there is less phase space available in the center of the triangle, hence even a totally ergodic wavefunction would have a smaller amplitude in this region. (b) The projection of the wavefunction shown in Fig. 3b. Comparing (a) and (b), one can appreciate the term "scarred wavefunction."

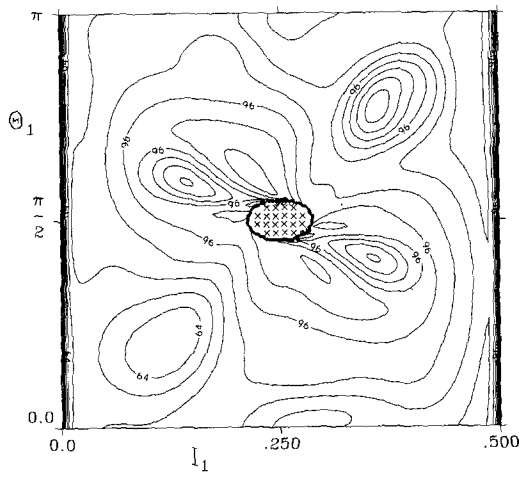

(a)

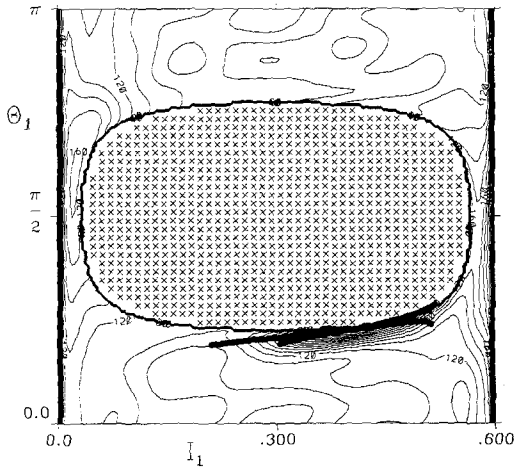

(b)

Fig. 5. (a) The energy-averaged QSOS for all 40 states in the quasichaotic energy range. This QSOS is relatively smooth (compare with Fig. 1f), but one can see the imprint of the invariant tori and the $I_0 = 0$ and $I_1 = 0$ periodic orbits along the $I_1 = 0$ and $I_1 = 0.5$ lines. (b) The energy-averaged QSOS for all 29 states in the chaotic energy range. Here again the most prominent features are localization around the shortest periodic orbits ($I_0 = 0$, $I_1 = I_2$, and $I_1 = 0$). The stable and unstable manifolds are shown as circles for the $I_1 = I_2$ periodic orbit.

by examining the QSOS. After such an examination, it was clear that almost all states were supported by only a few classical structures, and that only two were ergodic.

For example, Fig. 3b shows a scarred state near a quantizing energy. Unlike the scarred states in the quasichaotic regime, this state is not completely on the SUM of the scarring orbit (which includes the entire $I_1 = 0.5$ line), but is also localized on another classical structure (clearly visible in other states) not associated with that periodic orbit. However, a typical scarred state in the antiscarring interval (Fig. 3c) is far less localized than the one in the scarring interval. Finally, in Fig. 3d we show the most ergodic states in the energy interval, which would (as with Fig. 1f) be ergodic after smoothing.

These observations indicate that there is a hierarchy of localization. Those states in the quasichaotic region and near an energy which quantizes the action are completely localized on the SUM of the quantized periodic orbit; the others not close to the quantizing energy are supported by two or more orbits. In the chaotic region, scarred states near the quantizing energy are mostly localized on the scarring SUM, but have a noticeable fraction off of that manifold. Finally, those in the chaotic region but not near a quantizing energy have at least two states equally contributing.

Finally, we look at energy-averaged QSOS. The expectation from the work of Berry and Bogomolny is that if we average over an energy interval that is small classically (i.e., the classical dynamics changes very little), but quantum mechanically large (containing many states), we should see a smooth background and the contributions due to the shortest periodic orbits. To verify this, we averaged the QSOS with equal weights over the energy interval that includes one scarring and one antiscarring region. The results are shown in Fig. 5a for the quasichaotic states and Fig. 5b for the chaotic states. Indeed, in both cases the shortest periodic orbits can clearly be seen. We expect that as N increases, averaging more states over the same energy interval would lead to smoother distributions, and even the localization due to the shortest periodic orbits would disappear.

9. CONCLUSION

In conclusion, we return to our original question: can we say anything about energy eigenfunctions of nonintegrable systems without solving the Schrödinger equation and using only the knowledge of the classical system? The answer is yes, but not as originally expected. Energy-averaged eigenstates give good agreement with Wigner or Husimi distributions evenly spread over phase space. On the other hand, most individual states are strongly influenced by only a few classical structures (i.e., tori or SUM

of unstable periodic orbits). The details of the morphologies of these states are given by the EBK approximation (for states localized on tori) or the work of Bogomolny and Berry (for states localized on a periodic orbit). However, we cannot say precisely which states will be scarred, but can only say that the most dramatic localization occurs at energies which nearly quantize the unstable periodic orbit, and that scarred states in an anti-scarring energy interval are supported by more than just one orbit.

We also find that the localization is more pronounced in the quasichaotic regime than in the completely chaotic regime. This is consistent with the work of Alhassid and co-workers,[66] which showed that the distribution of the matrix elements between eigenvectors is a χ^2 distribution with ν degrees of freedom. If the classical limit is completely chaotic, $\nu = 1$; however, if there is a region of regular motion, $\nu < 1$, and therefore the distribution gives rise to greater fluctuations in the matrix elements.

Given this unexpectedly high degree of order in the eigenstates, one wonders whether there is a qualitative difference between eigenstates of chaotic Hamiltonians and those of integrable Hamiltonians (compare Figs. 1b and 1c). The answer may lie in recent work by Leboeuf and Voros,[18] who have shown that the zeros of the Husimi distribution are qualitatively different for these two classes of systems, and are therefore an unmistakable signature of the classical dynamics in the quantum system.

ACKNOWLEDGMENTS

The author gratefully acknowledges the support of the Roland H. O'Neal Professorship and the National Science Foundation under grant PHY-9009769.

REFERENCES

1. G. Casati, B. V. Chirikov, I. Guarneri, and D. L. Shepelyansky, *Phys. Rev. Lett.* **56**:2437 (1986).
2. M. C. Gutzwiller, *J. Math. Phys.* **8**:1979 (1967); **10**:1004 (1969); **11**:1791 (1970); **12**:343 (1971).
3. R. Balian and C. Bloch, *Ann. Phys. (N.Y.)* **69**:76 (1972).
4. E. J. Heller, *Phys. Rev. Lett.* **53**:1515 (1984).
5. M. V. Berry, in *Chaotic Behavior of Deterministic Systems*, G. Iooss, R. G. H. Helleman, and R. Stora, eds. (North-Holland, Amsterdam, 1983).
6. M. V. Berry and K. E. Mount, *Rep. Prog. Phys.* **35**:315 (1972).
7. M. Tabor, *Chaos and Integrability in Nonlinear Dynamics* (Wiley, New York, 1989); A. M. Ozorio de Almeida, *Hamiltonian Systems: Chaos and Quantization* (Cambridge University Press, Cambridge, 1988); L. E. Reichl, *The Transition to Chaos in Conservative Classical Systems: Quantum Manifestations* (Springer-Verlag, Berlin, 1992); M. C. Gutzwiller, *Chaos in Classical and Quantum Mechanics* (Springer-Verlag, New York, 1990); B. Eckhardt, *Phys. Rep.* **163**:205 (1988).
8. V. I. Arnol'd, *Mathematical Methods of Classical Mechanics* (Springer-Verlag, New York,

1978); A. J. Lichtenberg and M. A. Lieberman, *Regular and Stochastic Motion* (Springer-Verlag, New York, 1983); R. S. MacKay and J. D. Meiss, eds., *Hamiltonian Dynamical Systems: A reprint selection* (Adam Hilber, Bristol, 1987); R. Z. Sagdeev, D. A. Usikov, and G. M. Zaslavsky, *Nonlinear Physics: From the Pendulum to Turbulence and Chaos* (Harwood Academic Publishers, Chur, 1988).

9. V. I. Arnol'd, *Mathematical Methods of Classical Mechanics* (Springer-Verlag, New York, 1978), Chapter 10.
10. J. H. Van Vleck, *Proc. Natl. Acad. Sci. USA* **14**:178 (1928).
11. V. P. Maslov and M. V. Fedoriuk, *Semiclassical Approximation in Quantum Mechanics* (Reidel, Dordrecht, 1981).
12. M. V. Berry, in *Lectures at Les Houches 1980, Session XXXV, Physics of Defects*, R. Balian, M. Kleman, and J. P. Poirier, eds. (North-Holland, Amsterdam, 1981).
13. E. P. Wigner, *Phys. Rev.* **40**:749 (1932).
14. A. O. de Almeida and J. H. Hannay, *Ann. Phys. (N.Y.)* **138**:115 (1982).
15. K. Husimi, *Proc. Phys. Math. Soc. Jpn.* **22**:264 (1940).
16. A. Perelomov, *Generalized Coherent States* (Springer-Verlag, Berlin, 1986); W.-M. Zhang, D. H. Feng, and R. Gilmore, *Rev. Mod. Phys.* **62**:867 (1990), J. Kurchan, P. Leboeuf, and M. Saraceno, *Phys. Rev. A* **40**:6800 (1989); L. G. Yaffe, *Rev. Mod. Phys.* **54**:407 (1982).
17. K. Takahashi and N. Saitô, *Phys. Rev. Lett.* **55**:645 (1985).
18. P. Leboeuf and A. Voros, *J. Phys. A: Math. Gen.* **23**:1765 (1990).
19. M. V. Berry, *J. Phys. A* **10**:2083 (1977); A. Voros, in *Stochastic Behavior in Classical and Quantum Hamiltonian Systems*, G. Casati and J. Ford, eds. (Springer, Berlin, 1979).
20. E. J. Heller, *Phys. Rev. A* **35**:1360 (1987).
21. A. Schnirelman, *Usp. Mat. Nauk* **29**:181–182 (1974); S. Zelditch, Preprint (1984); Y. Colin de Verdiere, *Commun. Math. Phys.* **102**:497–502 (1985).
22. S. W. McDonald, Ph.D. thesis, University of California, Lawrence Berkeley Laboratory, 1983 [Report No. LBL-14837], unpublished; S. W. McDonald and A. N. Kaufman, *Phys. Rev. Lett.* **42**:1189 (1979).
23. R. L. Waterland, J.-M. Yuan, C. C. Martens, R. E. Gillilan, and W. P. Reinhardt, *Phys. Rev. Lett.* **61**:2733 (1988).
24. M. Feingold, R. G. Littlejohn, S. B. Solina, and J. S. Pehling, *Phys. Lett. A* **146**:199 (1990).
25. E. B. Bogomolny, *Physica D* **31**:169 (1988).
26. M. V. Berry, *Proc. R. Soc. Lond. A* **423**:219 (1989).
27. M. V. Berry and M. Tabor, *Proc. R. Soc. A* **349**:101 (1976).
28. M. C. Gutzwiller, *Phys. Rev. Lett.* **45**:150 (1980); M. C. Gutzwiller, *Physica D* **5**:183 (1982).
29. D. Wintgen, *Phys. Rev. Lett.* **61**:1803 (1988).
30. L. S. Schulman, *Techniques and Applications of Path Integration* (Wiley-Interscience, New York, 1981).
31. S. C. Creagh, J. M. Robbins, and R. G. Littlejohn, *Phys. Rev. A* **42**:1907 (1990); B. Eckhardt and D. Wintgen, *J. Phys. A: Math. Gen.* **24**:4335 (1991); J. M. Robbins, *Nonlinearity* **4**:343 (1991).
32. S. Creagh and R. G. Littlejohn, *Phys. Rev. A* **44**:836 (1991).
33. P. Cvitanovic and B. Eckhardt, *Phys. Rev. Lett.* **63**:823 (1989); P. Cvitanovic, *Phys. Rev. Lett.* **61**:2729 (1988).
34. M. V. Berry and J. P. Keating, *J. Phys. A: Math. Gen.* **23**:4839 (1990).
35. M. Sieber and F. Steiner, *Phys. Rev. Lett.* **67**:1941 (1991).
36. G. Tanner, R. Scherer, E. B. Bogomolny, B. Eckhardt, and D. Wintgen, *Phys. Rev. Lett.* **67**:2410 (1991).

37. S. Tomsovic and E. J. Heller, *Phys. Rev. Lett.* **67**:664 (1991).
38. D. Wintgen and A. Honig, *Phys. Rev. Lett.* **63**:1467 (1989).
39. A. Ozorio de Almeida, *Nonlinearity* **2**:519 (1989).
40. D. Biswas, M. Azam, and S. V. Lawande, *Phys. Lett. A* **155**:117 (1990).
41. T. A. Brody, J. Flores, J. B. French, P. A. Mello, A. Pandey, and S. S. M. Wong, *Rev. Mod. Phys.* **53**:385 (1981).
42. O. Bohigas and M.-J. Giannoni, in *Mathematical and Computational Methods in Nuclear Physics*, J. S. Dehesa, J. M. G. Gomez, and A. Polls, eds. (Springer-Verlag, Berlin, 1983).
43. O. Bohigas, M.-J. Giannoni, and C. Schmidt, *Phys. Rev. Lett.* **52**:1 (1984).
44. D. Biswas and S. Jain, *Phys. Rev. A* **42**:3170 (1990).
45. P. Šeba and K. Zyczkowski, *Phys. Rev. A* **44**:3457 (1991).
46. M. Saraceno, *Ann. Phys. (N.Y.)* **199**:37 (1990); A. M. Ozorio de Almeida and M. Saraceno, *Ann. Phys. (N.Y.)* **210**:1 (1991).
47. N. L. Balazs and A. Voros, *Ann. Phys. (N.Y.)* **190**:1 (1989).
48. R. Aurich and F. Steiner, *Physica D* **48**:445 (1991).
49. M. Kuś, J. Zakrzewski, and K. Zyczkowski, *Phys. Rev. A* **43**:4244 (1991).
50. R. V. Jensen, M. M. Sanders, M. Saraceno, and B. Sundaram, *Phys. Rev. Lett.* **63**:2771 (1989).
51. D. Delande, in *Proceedings of Les Houches Summer School, Session LII*, A. Voros, M. Giannoni, and J. Zinn-Justin, eds. (Elsevier, Amsterdam, 1991).
52. H. Frisk, *Physica Scripta* **43**:545 (1991).
53. B. Eckhardt, G. Hose, and E. Pollak, *Phys. Rev. A* **39**:3776 (1989).
54. M. Shapiro, D. D. Taylor, and P. Brumer, *Chem. Phys. Lett.* **106**:325 (1984).
55. S. W. McDonald and A. N. Kaufman, *Phys. Rev. A* **37**:3067 (1988).
56. E. J. Heller, in *Quantum Chaos and Statistical Nuclear Physics*, T. H. Seligman and H. Nishioka, eds. (Springer-Verlag, Berlin, 1986).
57. P. O'Connor and E. J. Heller, *Phys. Rev. Lett.* **61**:2288 (1988).
58. E. J. Heller, P. W. O'Connor, and J. Gehlen, *Physica Scripta* **40**:354 (1989); P. O'Connor, J. Gehlen, and E. J. Heller, *Phys. Rev. Lett.* **58**:1296 (1987).
59. S. Sridhar, *Phys. Rev. Lett.* **67**:785 (1991).
60. H. J. Lipkin, M. Meshkov, and A. J. Glick, *Nucl. Phys.* **62**:188 (1965).
61. S. Y. Li, A. Klein, and R. M. Dreizler, *J. Math. Phys.* **11**:975 (1970).
62. P. Leboeuf and M. Saraceno, *J. Phys. A: Math. Gen.* **23**:1745 (1990).
63. P. Leboeuf and M. Saraceno, *Phys. Rev. A* **41**:4614 (1990).
64. D. C. Meredith, S. E. Koonin, and M. R. Zirnbauer, *Phys. Rev. A* **37**:3499 (1988).
65. P. Leboeuf, D. C. Meredith, and M. Saraceno, *Ann. Phys.* **208**:333 (1991).
66. Y. Alhassid and R. D. Levine, *Phys. Rev. Lett.* **57**:2879 (1986); Y. Alhassid and M. Feingold, *Phys. Rev. A* **39**:374 (1989).
67. For numerical methods to find periodic orbits, see M. Baranger and K. T. R. Davies, *Ann. Phys.* **186**:95 (1988).